# Web Supplement to Krukowski and Miller, *Nature Neuroscience* 4, 424-430 (2001)

In this supplement we present three additions to our paper:

1. Details of computational methods;
2. Studies of the effects of NMDA blockade;
3. A Simple Analytic Model of Simple Cell Responses

## 1 Details of Computational Methods

The model used in our study is in almost all essential details identical to the "computational" model described in Troyer et al.[1], except that NMDA receptors and synaptic depression were not considered in that study. Here we present all differences from the Methods described in Troyer et al.[1].

### LGN inputs and Thalamocortical Receptive Fields

We model X-cell inputs as in Troyer et al.[1], except that we use the data of Sclar[2] to determine the first harmonic (F1) of the LGN responses to a given contrast and temporal frequency (the data used in Troyer et al.[1] did not vary temporal frequency). Sclar[2] reports the F1's of the response of a typical LGN X-cell at multiple contrasts (80,40,20 and 10%) and multiple temporal frequencies (0.5, 1, 2, 4, 8, 16, 32 Hz). For other levels of contrast or temporal frequency, MATLAB's 2-D cubic interpolation (interp2) was used to interpolate the F1 value.

The pattern of thalamocortical input to simply cells was determined using the "broadly-tuned" receptive field parameters of Troyer et al.[1]. These parameters were chosen to make intracellular voltage modulations match the measured orientation tuning width of the voltage modulations of cortical simple cells[3].

### Model of NMDA conductances

While the non-NMDA time-varying conductances in the model (AMPA, GABA-A and adaptation) are modeled as a simple difference of single exponentials, as described in Troyer et al.[1], the decay of the NMDA conductance was modeled as a double exponential with a fast and a slow time constant:

$$g_{\mathrm{NMDA}}(t) = \sum_{t_j<t} \bar{g}_{\mathrm{NMDA}}(V_{\mathrm{shadow}}) \left( f_{\mathrm{fast}} e^{-(t-t_j)/\tau^{\mathrm{fall}}_{\mathrm{NMDA,fast}}} + (1-f_{\mathrm{fast}}) e^{-(t-t_j)/\tau^{\mathrm{fall}}_{\mathrm{NMDA,slow}}} - e^{-(t-t_j)/\tau^{\mathrm{rise}}_{\mathrm{NMDA}}} \right) \tag{1}$$

The sum is over presynaptic spike times $t_j$, and $f_{\text{fast}}$ represents the contribution of the faster exponential to the total decay term. $V_{\text{shadow}}$ is the membrane potential if spiking is ignored. That is, when the voltage reaches spike threshold, the actual voltage of the cell is held at $V_{\text{reset}}$ for a refractory period and then evolves from that level; but $V_{\text{shadow}}$ is never reset and evolves continuously as if no spike had occurred. We chose to use $V_{\text{shadow}}$ as the voltage controlling the voltage-dependent behavior of NMDA conductances for two reasons: (1) to avoid discontinuities in synaptic currents during spiking events; (2) to reflect the fact that NMDA conductances are on the dendrites, so that it is appropriate to link them to a voltage that reflects the net synaptic input and is not limited by spike threshold. Parameters were taken from the data for adult rats in a developmental study of NMDA conductances in the rat visual cortex[4]: $\tau^{\text{fall}}_{\text{NMDA,fast}} = 63\ msec$, $\tau^{\text{fall}}_{\text{NMDA,slow}} = 200\ msec$, $f_{\text{fast}} = 88\%$. We chose $\tau^{\text{rise}}_{\text{NMDA}} = 5.5msec$ to set the 10-90% rise time of the NMDA EPSC to be equal to $7.8msec$ as has been observed experimentally[5]. For the model of temporal frequency tuning of younger animals, we held the time constants fixed, and only adjusted the contribution of the faster time constant, as suggested by Carmignoto and Vicini[4] ($f_{\text{fast,young}} = 10\%$). We did not adjust $\tau^{\text{rise}}_{\text{NMDA}}$ for this case, as it only increased the 10-90% rise time slightly ($9.3msec$).

The voltage dependence of $\bar{g}_{\text{NMDA}}$ followed the model described in Jahr and Stevens[6]:

$$\bar{g}_{\text{NMDA}}(V) = 1/\frac{1 + (a_1(V) + a_2(V,C))(a_1(V)B_1 + a_2(V,C)B_2)}{[Aa_1(V)((b_1(V) + B_1) + Aa_2(V,C)(b_2(V) + B_2)]} \tag{2}$$

Here, the lower-case parameters depend on voltage $V$, in units of $mV$, and $a_2$ also depends on magnesium concentration $C$, in units of $uM$. Parameters are as follows: $a_1(V) = e^{(-0.016V - 2.91)}msec^{-1}$, $a_1(V,C) = Ce^{(-0.045V - 6.97)}uM^{-1}msec^{-1}$, $b_1(V) = e^{(0.009V + 1.22)}msec^{-1}$, $b_2(V) = e^{(0.017V + 0.96)}msec^{-1}$, $A = e^{(-2.847)}msec^{-1}$, $B_1 = e^{(-0.693)}msec^{-1}$, $B_2 = e^{(-3.101)}msec^{-1}$, $C = 100uM$. With this model of voltage dependence, the NMDA channels are still 35.5% open at the model spike threshold voltage, $-52.5mV$ (figure 1a). In response to a high contrast optimal grating, $V_{\text{shadow}}$ reaches a peak of approximately -46 mV, where the NMDA channels are 43.8% open.

Figure 1b compares two measures of the relative strength of NMDA and AMPA conductances. One, the NMDA/AMPA amplitude ratio (horizontal axis of Fig. 1b) was used by Crair and Malenka[7]. This is the ratio of the amplitude of NMDA EPSC's with the cell held at +40mV to the amplitude of AMPA EPSC's with the cell held at -90mV. The other, the %NMDA integrated current (vertical axis of Fig. 1b), is the percent of the temporally-integrated current (*i.e.*, of the total charge transfer) through excitatory conductances that is mediated by NMDA conductances, when the postsynaptic cell is clamped at the spike-threshold voltage of -52.5 mV. As can be seen, even for relatively modest NMDA/AMPA amplitude ratios, the integrated current is dominated by NMDA, due to the long NMDA decay-time constants.

Since the main parameter we use to set synaptic strengths is the total integrated current (see below), we use the % of the integrated current that is mediated by NMDA to describe the relative

strengths of NMDA and AMPA conductances. Crair and Malenka[7] report an NMDA/AMPA amplitude of 0.30 for the oldest thalamocortical slices that they studied (8 to 14 postnatal days) which corresponds to 91.2% of the integrated current mediated by NMDA. We have accordingly used 90% NMDA as our default for full strength of NMDA in thalamocortical synapses. When we use young NMDA, we compute integrated current using the young NMDA parameters.

## Synaptic Depression

We use a simple model for synaptic depression, described previously[8,9], that uses only two parameters: $f$ ($0 \leq f \leq 1$), the factor by which the efficacy of a synapse gets scaled immediately after a spike, and $\tau$, the time constant of an exponential decay back to maximum efficacy. We define a scaling factor, $A(t) \leq 1$, as the ratio of the efficacy at time $t$ to the maximum efficacy; the conductance opened by a synapse due to a presynaptic spike at $t$ is scaled by $A(t)$. Depression is implemented by storing, for each presynaptic cell, the most recent time of spiking and the most recent scaling factor. Scaling factors then only have to be updated at the moment of each presynaptic spike, using the iterative equation $A(t_i) = 1 - [1 - A(t_{i-1})f] \exp(-(t_i - t_{i-1})/\tau)$, where $t_i$ is the current spike time and $t_{i-1}$ is the time of the most recent spike. We used parameters determined from paired-pulse experiments that were performed on putative thalamocortical (tc) synapses onto cells in layer 4[10] ($\tau_{\mathrm{tc}} = 99$ msec, $f_{\mathrm{tc}} = 0.563$) and intracortical (ic) synapses within layer 4[11] ($\tau_{\mathrm{ic}} = 57$ msec, $f_{\mathrm{ic}} = 0.875$; see Kayser et al.[12] for details on parameters found in the literature using different experimental protocols.) Synaptic depression was not included in the intracortical I⇒E synapses.

## Parameter Sets

All parameters are identical to the default parameters of the computational model of Troyer et al.[1], with the following exceptions:

1. The amplitude of the adaptation conductance, $\bar{g}_{\mathrm{adapt}}$, was reduced by a factor of 5 from a value of 3 nS to 0.6 nS, to obtain more realistic firing rates as discussed in Troyer et al.[1]. We have tested that this decreased level of adaptation gives reasonable levels of gain, as measured from plots of firing rates versus injected current and from plots of firing rate versus instantaneous membrane potential.

2. All cells in the model, both excitatory and inhibitory, receive a constant rate of Poisson-process, AMPA-mediated background input so that, when combined with background firing rates of LGN cells, cortical cells have appropriate background firing rates of approximately 0.5Hz for excitatory cells and 20-30Hz for inhibitory cells. The parameters of this background had to be changed from Troyer et al.[1] to compensate for the changes induced by NMDA and synaptic depression. Without synaptic depression, the unitary conductance had an amplitude

.89 nS, and the rate of the Poisson process was 6000Hz. With synaptic depression, the unitary conductance had an amplitude 7.12 nS, and the rate of the Poisson process was 500Hz.

3. As described in Troyer et al.[1], the three main parameters that controlled the behavior of the model were the total synaptic strengths for the thalamocortical synapses (onto either excitatory or inhibitory cortical cells), the intracortical excitatory synapses and the intracortical inhibitory synapses. These are measured as the integrated current at threshold voltage when all the synapses onto a cell are simultaneously activated once. With no synaptic depression, these were: thalamocortical excitation = 5 nA msec, intracortical inhibition = 3.5 nA msec, intracortical excitation = 4 nA msec. With synaptic depression, these were: thalamocortical excitation = 20 nA msec, intracortical inhibition = 5 nA msec, intracortical excitation = 7 nA msec. Synaptic strengths needed to be increased when including synaptic depression, since the synapses begin in an intermediate state of depression due to the background firing of the presynaptic cells. Thalamocortical synapses need a stronger increase than intracortical synapses, because LGN cells have much higher background firing rates than intracortical cells. For simulations with no feedback excitatory connections, the intracortical excitation strength was simply set to 0. As mentioned above, note that changing the proportion of NMDA in any of the categories of excitatory synapses (thalamocortical⇒E, thalamocortical⇒I, or intracortical excitatory) does not change the total synaptic strength, but only changes the percentage of the total integrated threshold current that is mediated by NMDA versus AMPA.

## Simulations

Simulations were implemented as described in Troyer et al.[1], with a few subtle modifications. Stimulus presentations were all for one second, regardless of temporal frequency. A "blank screen" was run for one second preceeding each stimulus presentation to allow the network to achieve stability before the stimulus was presented. Background and stimulus-induced output statistics were determined from the second half-second of the "blank screen" and stimulus presentations, respectively, again to allow the network to first achieve steady-state which, when including NMDA, took on the order of a few hundred milliseconds.

All population results, such as temporal frequency tuning curves, were determined by averaging over the pool of excitatory cells with preferred orientation $\pm 2.5^o$ about the stimulus orientation (this bin included 35 excitatory cells and 10 inhibitory cells). The cutoff temporal frequency was determined by taking the mean stimulus-induced firing rates (subtracting off background firing rates) for these excitatory cells at a series of temporal frequencies (1, 2, 4, 6, 8, 12, 16, 24 and 32Hz) and using matlab's 1-D cubic spline interpolation routine, "interp1," to find the lowest frequency above the preferred frequency at which the response reaches half of the maximal response.

## 2 Studies of the effects of NMDA blockade

To study the effect of NMDA blockade on temporal frequency tuning, we fixed the fraction of excitatory currents mediated by NMDA in the different excitatory connections in the absence of blockade, and then reduced the strength of NMDA conductances by different factors, mimicking different levels of pharmocological antagonism. We implemented this blockade in two different ways. With "global" blockade, all NMDA conductances throughout the network were reduced, mimicking pumping NMDA antagonists throughout a local region of cortex. With "local" blockade, NMDA conductances were reduced only in the synapses onto a single cell, while all other cells in the network received full strength NMDA conductances, mimicking local iontophoresis of or intracellular delivery of a pharmacological agent.

The effect of global blockade of NMDA on temporal frequency tuning depends on which synapses have NMDA. Weak blockade of NMDA suddenly turns off the feedback amplifier, which had selectively amplified the lower frequencies. This somewhat increases the cutoff frequency, whether there is NMDA in thalamocortical synapses onto both excitatory and inhibitory cells or only onto excitatory cells (figure 2, % NMDA Blockade $< 30\%$). However, higher levels of NMDA blockade may either raise or lower the cutoff frequency, depending respectively on whether there is NMDA in thalamocortical synapses onto both excitatory and inhibitory cells or onto excitatory cells alone. With thalamocortical NMDA onto both excitatory and inhibitory cells, increasing levels of NMDA blockade simply eliminate the effects of NMDA, revealing the AMPA-mediated temporal frequency tuning curve; this increases the high-frequency cutoff. With thalamocortical NMDA onto excitatory cells alone, however, the total inhibitory strength is unchanged by NMDA blockade, and only excitation is reduced. The effect is to "pull down" the tuning curve, without significantly changing its overall shape except that the weakest responses at high frequency become subthreshold. The high frequency cutoff, therefore, is actually lowered with increasing levels of NMDA blockade in this case.

When NMDA is blocked locally, on a single cell, the blocked cell receives feedback excitatory input from a network of cells that are low-pass tuned because their levels of NMDA are unaffected. This low-pass tuned feedback dominates at all levels of blockade, even though only the AMPA component of the feedback connections directly acts on the cell under study. As a result, the effect of local blockade is, again, simply to "pull down" the tuning curves, raising the effective threshold but otherwise leaving the shape of the feedback input unchanged. The temporal frequency cutoff, therefore, lowers slightly with increasing levels of blockade (figure 2).

## 3 A Simple Analytic Model of Simple Cell Responses

To test the intuitions of the effect of NMDA conductances acting as a low-pass filter in the thalamocortical connections, we implemented a simple analytic model of simple cell responses, which

we compare to the results of the detailed, network model. We consider the response of an excitatory simple cell to a drifting grating stimulus of its preferred orientation and spatial frequency with temporal frequency $f$. We let $L(t)$ be the mean rate of LGN input spiking to the cell, as a function of time, in response to this stimulus. $L(t)$ is periodic with period $2\pi/f$. We consider the cell to receive antiphase inhibition from an inhibitory simple cell receiving LGN input $L_{\rm inh}(t)$ that is identical except $180^o$ out of phase: $L_{\rm inh}(t) = L(t + \pi/f)$.

We ignore reversal potential effects, and model synapses as injecting currents. We consider three anatomical types of synapses: *el*, LGN→exc. cell; *il*, LGN→inh. cell; *ie*, exc. cell →inh. cell. The excitatory synapses are of three types, $N_s$ (NMDA with a slow decay component), $N_f$ (NMDA with a fast decay component), or $A$ (AMPA), while we restrict consideration of inhibitory synapses to a single type, $G$ (GABA-A). We let $a$ stand for anatomical type and $g$ stand for conductance type. Following a presynaptic spike at time $t_0$, a synapse of type $(a, g)$ injects a current $w_a^g \frac{1}{\tau_a^g} \exp\left[-(t - t_0)/\tau_a^g\right]$ for $t \geq t_0$. Here, $w_a^g$ is the weight and $\tau_a^g$ the decay time of the synaptic type. These currents on cell type $c$, $c \in \{e, i\}$ (exc. or inh.), are converted to voltage by convolution with $\frac{R_c}{\tau_c} \exp\left(-t/\tau_c\right)$ where $\tau_c$ is the cell's membrane time constant and $R_c$ its input resistance. Replacing the actual spike train with the mean rate of spiking, the inhibitory cell's stimulus-induced voltage response $V_i$, subtracting off the background voltage response, is

$$V_i(t) = \frac{R_i}{\tau_i} \exp(-t/\tau_i) \star \sum_{g \in A, N_s, N_f} \frac{w_{il}^g}{\tau_{il}^g} \exp(-t/\tau_{il}^g) \star L(t + \pi/f) \tag{3}$$

Here, $\star$ indicates convolution.

We model each cell's spiking response $r_c(t)$ as $r_c(t) = [k_c(V_c(t) - V_c^{th}) + r_c^0]^+$ where $V_c$ is the cell's stimulus-induced voltage response, $r_c^0$ is the cell's firing rate in the absence of a stimulus, $k_c$ is the gain of the cell, $V_c^{th}$ is a threshold voltage, and $[]^+$ indicates rectification: $[x]^+ = x$, $x \geq 0$; $= 0$, otherwise. The parameters, $k_i$, $k_e$, $V_e^{th}$, and $V_i^{th}$ were fit to the instantaneous voltage and firing rate responses of cells in the full model in response to an optimal high contrast grating, with no amplifier, no thalamocortical NMDA and no synaptic depression (figure 3a and b). The fit parameters were $k_e$ =17 spikes/sec/mV, $k_i$ =20 spikes/sec/mV, $V_e^{th}$ =1 mV, $V_i^{th}$ =1.5 mV. (Note that this value for $k_e$ is larger than, but of a comparable magnitude as, the gain predicted by the linear threshold model of Carandini and Ferster[3] – 7.2 spikes/sec/mV – who comment that their model purposely picked a threshold on the low end of the range of thresholds observed for individual spikes, and compensated by lowering the gain parameter.) For the inhibitory cell, we simplify by assuming that $r_i^0$ is large enough that the spiking rate never rectifies. Since the fit value for inhibitory threshold was close to 0 mV, we simply write the stimulus induced inhibitory firing rate, with background firing rate subtracted off, as $r_i(t) = k_i V_i(t)$.

The excitatory cell's stimulus-induced voltage response is then

$$V_e(t) = \frac{R_e}{\tau_e} \exp(-t/\tau_e) \star \left[ \sum_{g \in N_s, N_f, A} \frac{w_{el}^g}{\tau_{el}^g} \exp(-t/\tau_{el}^g) \star L(t) - \frac{w_{ei}^G}{\tau_{ei}^G} \exp(-t/\tau_{ei}^G) \star r_i(t) \right] \tag{4}$$

$$= \frac{R_e}{\tau_e}\exp(-t/\tau_e) \star \left[ \sum_{g\in N_s,N_f,A} \frac{w_{el}^g}{\tau_{el}^g}\exp(-t/\tau_{el}^g) \star L(t) - \right.$$
$$\left. \frac{w_{ei}^G}{\tau_{ei}^G}\exp(-t/\tau_{ei}^G) \star \left( \frac{k_i R_i}{\tau_i}\exp(-t/\tau_i) \star \sum_{g'\in N_s,N_f,A} \frac{w_{il}^{g'}}{\tau_{il}^{g'}}\exp(-t/\tau_{il}^{g'}) \star L(t+\pi/f) \right) \right] \quad (5)$$

We assume that this voltage response is dominated by the mean or DC, and the first harmonic or F1 (the component at the temporal frequency of the grating stimulus). This assumption can be justified quite generally for simple cells with LGN inputs defined by a Gabor function with two or more subregions (T. Troyer, A. Krukowski and K.D. Miller, unpublished) and also is well satisfied in simulations. $L(t+\pi/f)$ has DC equal to, and F1 equal in magnitude but opposite in sign to, those of $L(t)$; call the latter $\mathrm{DC_L}$ and $\mathrm{F1_L}$ respectively. Each convolution with an exponential $\frac{1}{\tau}\exp(-t/\tau)$ multiplies the Fourier transform of the voltage at frequency $p$ by $1/(1+i2\pi p\tau)$, which multiplies the amplitude of the response at that frequency by $[1+(2\pi p\tau)^2]^{-\frac{1}{2}}$. Thus, the amplitudes of the DC and the F1 of the excitatory cell's voltage response are:

$$\mathrm{DC}_e = R_e \left[ \left( \sum_{g\in N_s,N_f,A} w_{el}^g - w_{ei}^G k_i R_i \sum_{g'\in N_s,N_f,A} w_{il}^{g'} \right) \mathrm{DC_L} \right] \quad (6)$$

$$\mathrm{F1}_e = \frac{R_e}{[1+(2\pi f\tau_e)^2]^{\frac{1}{2}}} \left[ \sum_{g\in N_s,N_f,A} \frac{w_{el}^g}{[1+(2\pi f\tau_{el}^g)^2]^{\frac{1}{2}}} \right.$$
$$\left. + \frac{w_{ei}^G}{[1+(2\pi f\tau_{ei}^G)^2]^{\frac{1}{2}}} \frac{k_i R_i}{[1+(2\pi f\tau_i)^2]^{\frac{1}{2}}} \sum_{g'\in N_s,N_f,A} \frac{w_{il}^{g'}}{\left[1+(2\pi f\tau_{il}^{g'})^2\right]^{\frac{1}{2}}} \right] \mathrm{F1_L} \quad (7)$$

All the parameters for the analytic model were matched to the corresponding parameters of the full model. The cellular input resistances and membrane time constants were set to the mean values from the full model during presentation of a high contrast grating: $R_e$ =23.8 MOhm, $\tau_e$ =11.9 msec, $R_i$ = 34.6 MOhm, $\tau_i$ =7.4 msec. Synaptic decay time constants depend only on synapse type, and not synapse location: $\tau^G = 5.25$ msec, $\tau^A = 1.75$ msec, $\tau^{N_f} = 63$ msec, $\tau^{N_s} = 200$ msec. Synaptic current weights are matched to the integrated threshhold current parameters of the full model. The inhibitory current is $w_{ei}^G = 3.5$ nA msec. The total thalamocortical synaptic weights onto either excitatory and inhibitory cells are $\sum_{g\in N_s,N_f,A} w_{el}^g = \sum_{g\in N_s,N_f,A} w_{il}^g = 5$ nA msec. The weights of the three types depend on the percentage current mediated by NMDA. For no NMDA, $w^A = 5$ nA msec, $w^{N_s} = w^{N_f} = 0$. For full strength 90% NMDA, $w^A = 0.5$ nA msec, $w^{N_s} = 1.4$ nA msec, $w^{N_f} = 3.1$ nA msec. The values of $\mathrm{F1_L}$, as a function of temporal frequency, were taken from the data of Sclar[2]. For each temporal frequency, $\mathrm{DC_L}$ was then calculated by assuming the F1 was generated from the addition of a sinusoid and a background firing rate of 12.5 Hz, rectified at 0.

To compare temporal frequency tuning curves from the analytic model to those generated from average stimulus-induced excitatory-cell firing rates from the full model, we calculated mean firing

rates by generating sinusoidal voltage traces with modulation amplitude equal to $F1_e$ and mean equal to $DC_e$, passing them through the linear threshold model with gain $k_e = 17$ spikes/sec/mV and threshold $V_e^{th}$ =1 mV, and taking the temporal average.

## References


[1] T. W. Troyer, A. Krukowski, N. J. Priebe, and K. D. Miller. Contrast-invariant orientation tuning in cat visual cortex: Feedforward tuning and correlation-based intracortical connectivity. *J. Neurosci.*, 18:5908–5927, 1998.

[2] G. Sclar. Expression of "retinal" contrast gain control by neurons of the cat's lateral geniculate nucleus. *Exp. Brain Res.*, 66:589–596, 1987.

[3] M. Carandini and D. Ferster. Membrane potential and firing rate in cat primary visual cortex. *J. Neurosci.*, 20:470–484, 2000.

[4] G. Carmignoto and S. Vicini. Activity-dependent decrease in NMDA receptor responses during development of the visual cortex. *Science*, 258,:1007–1011, 1992.

[5] R. A. Lester, J. D. Clements, G. L. Westbrook, and C. E. Jahr. Channel kinetics determine the time course of NMDA receptor-mediated synaptic currents. *Nature*, 346:565–567, 1990.

[6] C. E. Jahr and C. F. Stevens. Voltage dependence of NMDA-activated macroscopic conductances predicted by single-channel kinetics. *J. Neurosci.*, 10:3178–3182, 1990.

[7] M. C. Crair and R. C. Malenka. A critical period for long-term potentiation at thalamocortical synapses. *Nature*, 375, 1995.

[8] M. V. Tsodyks and H. Markram. The neural code between neocortical pyramidal neurons depends on neurotransmitter release probability. *Proc. Natl. Acad. Sci. USA*, 94, 1997.

[9] L. F. Abbott, J. A. Varela, K. Sen, and S. B. Nelson. Synaptic depression and cortical gain control. *Science*, 275:220–224, 1997.

[10] K. J. Stratford, K. Tarczy-Hornoch, K. A. Martin, N. J. Bannister, and J. J. Jack. Excitatory synaptic inputs to spiny stellate cells in cat visual cortex. *Nature*, 382:258–261, 1996.

[11] K. Tarczy-Hornoch. *Physiology of Synaptic Inputs to layer IV of Cat Visual Cortex.* PhD thesis, Oxford University, England, 1996.

[12] A. S. Kayser, N. J. Priebe, and K. D. Miller. Contrast-dependent nonlinearities arise locally in a model of contrast-invariant orientation tuning. *J. Neurophysiol.*, (submitted), 2000.

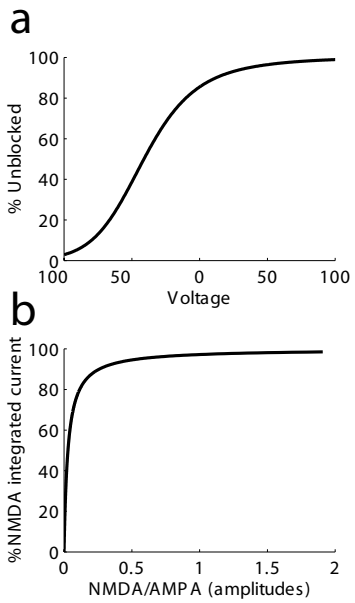


**Figure 1:**

(a) NMDA Voltage Dependence using the model from Jahr and Stevens[6]. Percentage of Model NMDA channels open as a function of membrane potential. (b) Comparison of two measures of relative strengths of NMDA and AMPA. X-axis is the ratio of the amplitude of NMDA EPSC with the cell held at +40mV to the amplitude of AMPA EPSC with the cell held at -90mV (the measure used by Crair and Malenka[7]). Y-axis is the percent of the temporally-integrated current (*i.e.*, of the total charge transfer) through excitatory conductances that is mediated by NMDA conductances, when the postsynaptic cell is clamped at the spike-threshold voltage.

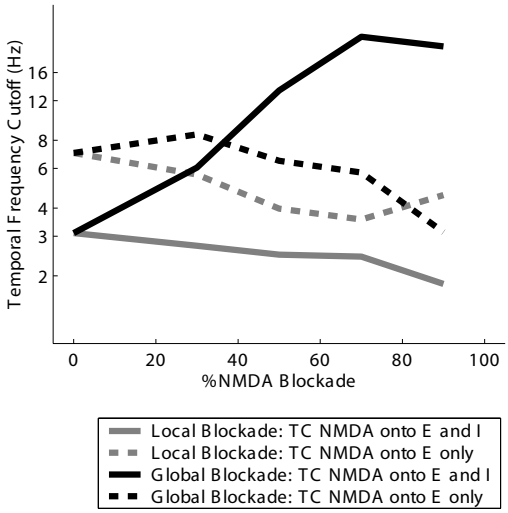


**Figure 2:**

Temporal frequency tuning of the model for different levels of NMDA blockade with the intracortical excitatory connections mediated by NMDA (95% of integrated current before blockade). Solid plots are with NMDA included in thalamocortical synapses onto both excitatory and inhibitory cells (90% of integrated threshold current for both before blockade). Dashed plots are with NMDA included in thalamocortical synapses onto excitatory cells only (90% of integrated threshold current before blockade), such that thalamocortical synapses onto inhibitory cells are purely AMPA mediated and are unaffected by the NMDA blockade. Black traces are for "global" NMDA blockade, where all NMDA connections throughout the network are reduced. Gray traces are for "local" blockade, where only the NMDA components of synapses onto a single cell are affected by the blockade, and all other connections within the network are unaffected.

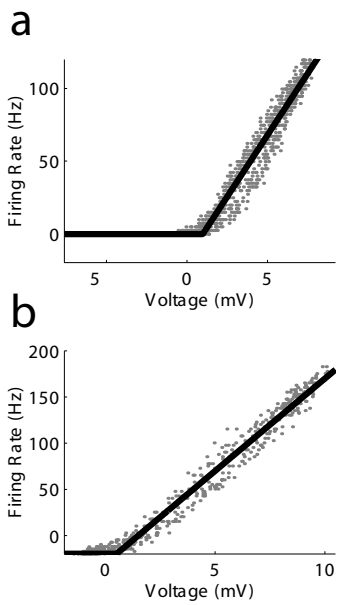


**Figure 3:**

Fitting a linear threshold spike rate model to the results of the full model. The dots represent instantaneous stimulus-induced (subtracting off background responses) voltages and firing rates of all the excitatory cells (a) and inhibitory cells (b) in the preferred orientation bin averaged over 20 presentations of a 2Hz, preferred orientation, high contrast grating, with no amplifier, no synaptic depression and 90% thalamocortical NMDA onto excitatory cells only. Black traces are the fits of the linear threshold model. The fit parameters, defined in the text, were, $k_e$ =17 spikes/sec/mV, $k_i$ =20 spikes/sec/mV, $V_e^{th}$ =1 mV, $V_i^{th}$ =1.5 mV. Note that the spike rates go below zero because they represent the rate above or below the background firing rate. The rectification of the linear threshold model occurs at the negative of the background firing rate (-0.7 Hz for excitatory cells and -19.6 Hz for inhibitory cells).